Construction and Building Materials 386 (2023) 131578

Contents lists available at ScienceDirect

Construction and Building Materials

journal homepage: www.elsevier.com/locate/conbuildmat

Statistical assessment of tensile and shear properties of unreinforced clay brick masonry

Lewis J. Gooch [a,*], Mark J. Masia [a], Mark G. Stewart [b], Chee Yin Lam [a]

[a] Centre for Infrastructure Performance and Reliability, The University of Newcastle Callaghan, NSW 2308, Australia
[b] Centre for Built Infrastructure Resilience School of Civil and Environmental Engineering, University of Technology Sydney Ultimo, NSW 2007, Australia

ARTICLE INFO

Keywords:
Unreinforced masonry
Finite element analysis
Material properties
Correlations
Probabilistic models

ABSTRACT

This paper presents the results of an extensive set of material characterisation tests performed on unreinforced clay brick masonry. The results of these experiments allow for the estimation of relationships between the measured material parameters. This study considers the relationships of flexural tensile bond strength to direct tensile bond strength, flexural to direct tensile strength of fired clay brick masonry units, and flexural tensile to shear bond strength. A mean ratio of flexural tensile bond strength to direct tensile bond strength of 2.06 and a COV of 31.5% were determined. For the flexural to direct tensile strength of fired clay brick masonry units, a mean ratio of 1.29 with a COV of 14.7% was estimated. Finally, considering the ratio of the shear bond to flexural tensile bond strengths, a mean ratio of 1.34 with a COV of 28.4% was found. In addition to these relationships, suitable probabilistic models were determined to describe the relationship between the flexural and direct tensile bond strengths, and the flexural tensile and shear bond strengths. These results may be used in future studies of URM structures, in particular finite element modelling and stochastic analyses of masonry.

1. Introduction

Masonry has remained a prominent construction material throughout history and is still widely used in modern construction. Unreinforced masonry (URM) is a composite material comprised of units; typically made of clay or concrete, bonded together with mortar; commonly made with cement, sand, and lime. This non-uniformity of geometry and materials results in a complex heterogeneous and anisotropic behaviour. While common masonry design and construction practices are well established through the application of simplified analytical models, the design and review of non-standard structures, as well as research applications, often requires the use of numerical modelling to examine a masonry structure's response to certain loading conditions.

A common form of numerical modelling is that of the finite element method (FEM). For modelling unreinforced masonry structures, the FEM may take the form of a macro-modelling or micro-modelling approach [1,15]. In the case of a macro-model, the masonry is considered to be a homogeneous material, with the properties of both the units and mortar being averaged and distributed across a continuum of elements. This approach is most common in larger structures or where the global response of the structure is of greater interest than distinct failure mechanisms.

Alternatively, a micro-modelling approach can be applied to incorporate the different responses of the units, mortar, and unit-mortar interfaces. A detailed micro-model will consider the geometry and behaviour of all three of these constituents. This modelling strategy, while the most accurate, is also highly computationally expensive. A simplified micro-model will reduce this limitation by incorporating the geometry of the mortar into the continuum of masonry units while maintaining the non-linear interface properties of the two. These three FE modelling techniques are presented in Fig. 1.

Perhaps the most important aspect in constructing an accurate masonry model is the allocation of accurate material properties. In the case of a micro-model, this is particularly relevant when assigning properties to the unit-mortar interface elements, as well as potential unit cracking interfaces, which are typically used to represent the non-linear response of an URM structure. To achieve this, numerical modelling of masonry is often complemented by material characterisation tests, either performed on the masonry under investigation or taken from literary sources.

Of the material properties relevant to the finite element (FE) modelling of URM masonry, the tensile and shear bond strength

* Corresponding author.
E-mail addresses: lewis.gooch@uon.edu.au (L.J. Gooch), mark.masia@newcastle.edu.au (M.J. Masia), mark.stewart@uts.edu.au (M.G. Stewart), cheeyin.lam@uon.edu.au (C.Y. Lam).

https://doi.org/10.1016/j.conbuildmat.2023.131578
Received 15 September 2022; Received in revised form 18 April 2023; Accepted 26 April 2023
Available online 4 May 2023

parameters govern the behaviour of perhaps the widest range of failure mechanisms, particularly those less favourable to URM structures. The sensitivity of a masonry model to these parameters is compounded by the fact that the tensile and shear bond strengths of a unit-mortar interface are highly variable, which may lead to non-conservatism in an FE model if suitable values are not adopted. Further to this, URM structures with relatively high mortar strength and low strength units, or those structures otherwise susceptible to failure through tensile unit cracking, require an accurate calibration of unit strength to adequately describe this failure mechanism.

As noted above, the high variability of URM properties compounds the difficulty of accurately estimating the structural capacity of an URM structure. Further to this, too simple a relationship between two material properties can lead to a poor representation of the true behaviour of a structure when modelled, numerically or analytically. An example of this is an URM shear wall with a high tensile bond strength, but a weak shear bond. This configuration is more likely to result in an unstable in-plane shear failure, while the adoption of the simplified relationship presented in AS 3700 [30], refer to Equation (1), will overlook this nuance and may predict the more stable in-plane flexural failure.

The current study investigates these sensitive material parameters through the consideration of their relationships with each other, as well as the statistical properties of these relationships. The creation of more accurate material relationships will then allow for the safety and reliability of current design guides and standards, such as AS 3700 [30], ASCE 41-13 [2] and NZSEE [19], to be examined, promoting more reliable standardised design methodologies. The investigation of the statistical properties of URM materials facilitates the application of accurate stochastic analyses of URM behaviour. This in turn allows for the determination of the capacity reduction factors, or partial safety factors, that will achieve the level of safety desired for masonry structures.

The material parameters that are the focus of this study, i.e.: the tensile and shear strengths of URM, are most relevant to the behaviour of masonry structures subjected to in-plane shear loading or out-of-plane bending. There have been a number of recent publications into the variability of these and other URM properties, as well as the influence this variability has on the resistance of URM walls. Isfeld et al. [11] applied similar material relationships to those presented in the current study, after the work of Van der Pluijm [35] and Milani and Lourenço [17], to calibrate reliability-based stochastic finite element analyses (SFEAs) of the out-of-plane bending capacity of URM walls. Additionally, Müller et al. [18], performed a similar investigation into the effect of spatially variable material properties on the compressive strength of both experimentally tested and numerically modelled URM walls. In both of these studies, it can be observed that consideration of the ratios and correlations between relevant material properties yields highly accurate numerical models.

2. Review of strength parameters

The strength parameters discussed above may be estimated through standard experimental testing. The flexural tensile bond strength for example can be estimated through the application of a bond wrench or beam bending test [30], the shear bond strength can be readily determined with an unconfined shear triplet test [7], and the flexural tensile unit strength, also known as the modulus of rupture, may be estimated with a beam bending test [26].

These interface properties may then be applied to the material models used to define the local responses within an FE model, as discussed below, or in simplified analytical models of URM. However, when applying such masonry models, the parameters adopted to define this behaviour must be representative of the failure mode being modelled. For example, the flexural tensile strength estimated through the application of a bond wrench test may not yield a value representative of a pure tensile failure mechanism, such as is shown in Fig. 2 due to the non-uniformity of tension when subjecting the specimen to combined bending and compression [35]. This may result in the adoption of properties inconsistent with the true behaviour of the material being adopted.

2.1. Tensile bond strength

Due to masonry's low tensile strength, the tensile bond strength of URM is perhaps one of the most important parameters to accurately estimate when performing either an FE or analytical analysis of masonry structures, particularly those subjected to in-plane lateral loads or out-of-plane bending, such as induced from wind- or seismic-events. However, the most common measure of tensile bond strength typically made in both laboratory and on-site tests is that of flexural tensile bond strength [19,31]. This presents an issue when assessing URM structures that may be subjected to direct tensile loading; a stress state commonly avoided in masonry, or when defining an FE material model calibrated based on uniform, direct tensile stresses. An example of this is the simple fracture energy-based model of tensile bond strength that may be adopted in the FE modelling software ABAQUS [1], as shown in Fig. 2. A similar, though more complex, mode of tensile behaviour is adopted in the FE modelling software DIANA, whereby an exponential softening is assumed [5].

It has been observed that direct and flexural tensile strengths are distinct in some materials such as plain concrete [21,30], and as such, one may expect a similar difference to appear in masonry. In the case of plain concrete, ratios of the flexural and direct tensile strengths between 1.35 [21] and 1.67 [29] have been observed, while a value equal to 1.5 is often utilised for masonry bond strength [35].

This distinction is difficult to attribute to a single cause, though it is likely due to two main attributes. Firstly, the effect of a strain gradient when concrete or masonry is subjected to flexural stresses ensures that failure will always initiate at approximately the same location within a specimen. This, unlike uniform tensile stress, reduces the effect of imperfections or weak spots across the cross-section of the specimen.

When a mortar joint or concrete cross-section is subjected to uniform tensile stress, failure will always initiate at a local defect within the specimen. This will result in a cascading material failure as the effective cross-section is reduced. This attribute is expected in both the heterogeneous cross-section of concrete and the highly variable bonded interface between a masonry unit and mortar. As a result, a tensile

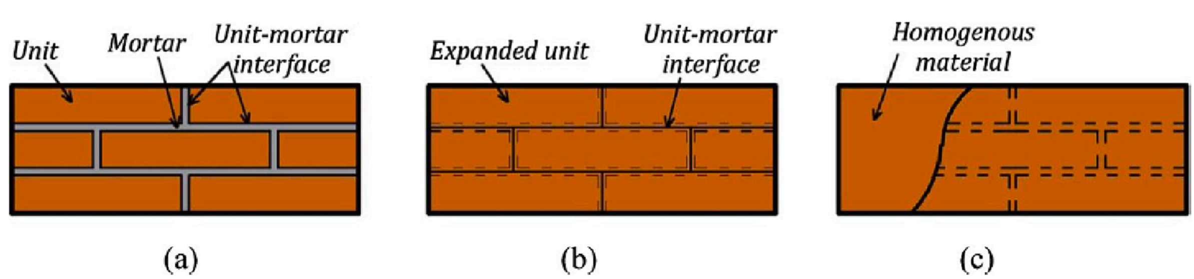

Fig. 1. Finite element modelling strategies: (a) detailed micro-model, (b) simplified micro-model, and (c) macro-model [1], after [15].

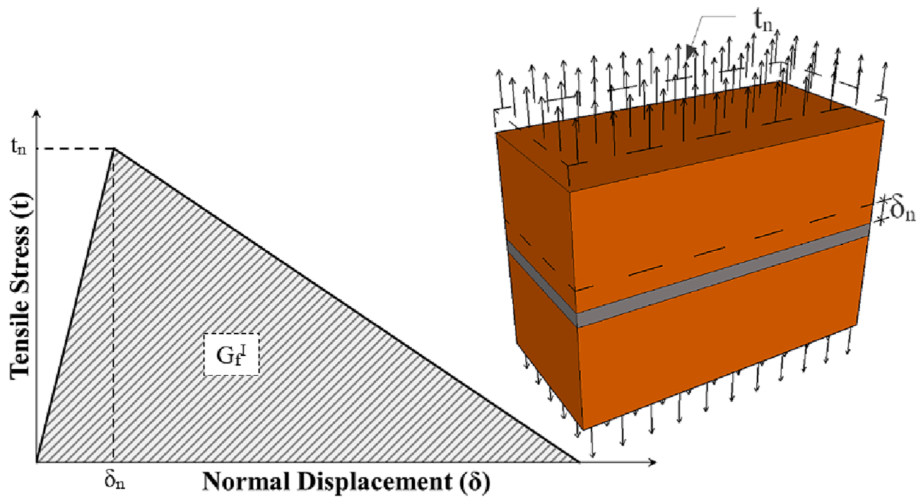

Fig. 2. Common tensile behaviour of unit-mortar interface as adopted in FE modelling. Adapted from Abdulla, et al. [1].

strength determined from a flexural tensile test, such as the bond wrench or beam test [30], would be expected to produce a higher strength capacity when compared to a direct tensile test, such as in Van der Pluijm [35] and the material models by Lourenço [15].

Another likely cause of this distinction is the inability to adequately apply a uniform tensile stress across the cross-section of either material. The presence of peaks in the stresses applied to a specimen will cause an underestimation of the stress required to initiate failure, as noted by Riddington and Jukes [23].

2.2. Unit tensile strength

The tensile strength of masonry units is a characteristic often ignored in standard analytical estimates of URM capacity given its tendency to outperform the mortar bond strength [19,29,31]. However, this property is necessary in the FE modelling of masonry structures and is critical to the assessment of some particularly unfavourable URM failure mechanisms, such as a diagonal tensile failure under in-plane shear loading, a particularly brittle and unstable failure mode which commonly includes failed masonry units [8,12].

As with the material model for tensile bond strength, the tensile behaviour of a masonry unit may be modelled using a simple fracture energy-based model [5], such as is shown in Fig. 3. Again, this material property is determined by an assumed uniform tensile stress applied to the cross-section of a unit. However, this stress distribution is not reflected by the modulus of rupture test specified by AS/NZS 4456.15 [26].

The failure of a masonry unit under either direct or flexural tensile stresses may again be similar to that of plain concrete, with a ratio of flexural to direct tensile strength of 1.5 being adopted in previous studies of masonry FEA behaviour [10,14,20] after the conclusions of Raphael [21] and Van der Plujim [35]. While masonry units are far more controlled than a mortar joint and perhaps more homogeneous than plain concrete, experimental testing indicates that the properties of clay brick masonry units maintain a high level of variability [9,14]. This, along with the causes outlined in Section 2.1, suggest that a measure of flexural tensile strength may not be adequate on its own to define the direct tensile models or behaviour of masonry units.

2.3. Shear bond strength

As with the tensile strength, the shear bond strength of the unit-mortar interface is an important material characteristic in the numerical and analytical assessment of masonry structures, particularly those

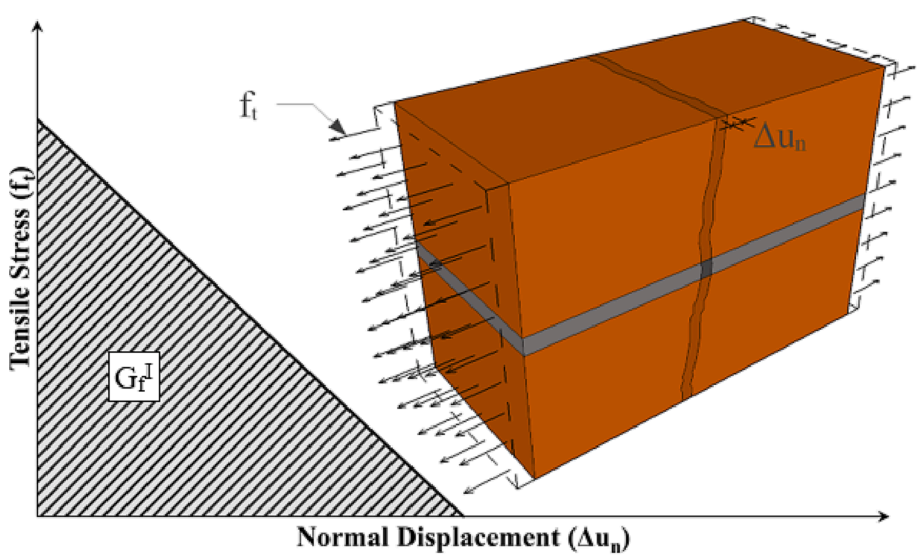

Fig. 3. Discrete cracking model of tensile unit behaviour interface as outlined by DIANA 10.3 [5].

subjected to in-plane shear failure [28]. However, unlike the aforementioned tensile strengths, the shear bond strength estimated using the triplet shear test [7] is directly analogous to the shear behaviour model adopted in FE packages such as ABAQUS and DIANA. Furthermore, previous studies provide recommendations regarding the correction of experimentally measured estimates of shear bond strength to account for a non-uniform distribution of stresses [22], as well as the failure bias between the two interfaces in a triplet test [13].

Despite this existing research and the relative certainty regarding the experimental estimation of shear bond strength, it is important to understand how this material characteristic interacts with other masonry properties. The current Australian Standard for masonry structures, AS 3700 [30], specifies the relationship between the flexural tensile and shear bond strengths shown in Equation (1), where f'_{ms} is the characteristic shear bond strength and f'_{mt} is the characteristic flexural tensile bond strength.

$$f'_{ms} = 1.25f'_{mt} \quad \text{for} \quad 0.15MPa \leq f'_{ms} \leq 0.35MPa \tag{1}$$

This relationship, examined in this paper and others [16], implies a fully correlated relationship between the shear and flexural tensile bond strengths, i.e.: ascertaining the flexural tensile strength of a mortar joint provides all of the shear bond strength properties of this same joint. While the assumption of some correlation between these properties is not unreasonable, as it may be expected that an increased tensile bond strength would indicate an increase in shear bond strength, as both properties are a function of the quality of the bond between mortar and the masonry unit, a full correlation between the two properties may not be reasonable. This distinction is especially important for the application of stochastic analyses. For example, the presence of a weak tensile strength and strong shear strength, or vice versa, in a URM wall subject to in-plane shear loading, may result in alternative modes of failure when compared to a structure with consistent measures of bond strength. This is also evident in the analytical expressions for in-plane shear failure modes found in design guides and standards [2,3,31].

3. Experimental testing

Experimental estimates of material properties were performed through the application of those testing methods noted in Section 2, as well as through two non-standard methods devised to examine the direct tensile strength of mortar joints and of masonry units. Tests were performed on a wide range of masonry combinations; up to four distinct clay masonry unit types combined with up to seven mortar mixes. In each combination case, several tests were performed in order to produce a reasonable mean strength estimate under the applied loading conditions. The mortar mixes chosen in this study as presented in Table 1. These mixes are based upon to the deemed-to-conform mortar compositions specified by AS 3700 [30], and are similar to the standardised mortar mix compositions presented in NZS 4210 [31], BS EN 1996-1-1 [3], CSA S304-14[4] and TMS 402/602-16 [34].

Table 1
Mortar properties adopted in laboratory tests.

Mortar Mix Designation	Mortar Mix (Cement: Lime: Sand)[1]	Joint Thickness (mm)
1	1:2:9	10
2	1:1:6	10
3	1:0:5[2]	10
4	1:0:5	10
5	1:0.5:4.5	10
6	1:0:4[2,3]	10
7	1:0:4	10

[1] Mortar ratios mixed by volume.
[2] Mortar mix did not include water thickener as recommended by AS3700 [30].
[3] Mortar mix was not used in the comparison of direct and flexural bond strengths.

It should be noted that, as the water thickener required by AS3700 [30] for mortar mixes without lime was reasonably difficult to source, mortar mixes of similar cement, lime, and sand ratios as those requiring this additive were constructed during the wait period for the thickener. These specimens, designated mixes 3 and 6, were then utilised in testing in order to compare their effectiveness and workability to the mixes that utilised the additive, namely, the mix designations 4 and 7. As mixes 3 and 6 were found to still be reasonably workable and produced results comparable to the other mixes utilised in this study, their results have been included in Section 4.

The selected sets of masonry units comprised, two types of extruded, cored, clay brick units and two types of pressed clay units. These units and their corresponding designations are presented in Fig. 4. All masonry units utilised in this testing program are of the standard Australian dimensions of 230 mm × 110 mm × 76 mm. Furthermore, both types of extruded unit have evenly spaced cores with diameters, or square side lengths for the Type 2 extruded units, of 30 mm and with edge distances of approximately 17 mm to both the header and stretcher faces of the unit. Both pressed units have a frog centred within the unit, with dimensions of approximately 145 × 41 mm. While standard unit dimensions vary somewhat internationally [25], the use of either extruded or pressed clay units is not uncommon.

3.1. Bond wrench test – flexural tensile bond strength

The bond wrench test outlined by AS3700 [30] was employed to estimate the flexural tensile bond strengths throughout this study. This test involves the creation of piers of masonry units, six units (five mortar joints) high in this study. The strength of each mortar joint is then estimated by clamping a wrench to the top unit of the pier and then gradually applying a moment until failure is achieved. The applied force, along with the masses and centres of mass of the unit and wrench is recorded such that a total moment at the point of failure may be estimated (see Equation (3)). A schematic diagram of the bond wrench setup is presented in Fig. 5. The flexural tensile bond strength, f_{sp}, is then estimated from Equation (2).

This test was selected in lieu of a beam bending test, such as is outlined in AS3700 [30], as the bond wrench test allows for a significantly faster test. This expedition was preferred given the large number of samples tested.

$$f_{sp} = \left(\frac{M_{sp}}{Z_d}\right) - \left(\frac{F_{sp}}{A_d}\right) \tag{2}$$

where M_{sp} is the applied bending moment about the centroid of the bedded area of the examined joint, estimated as per Equation (3), and Z_d is the section modulus of the bedded area about the axis about which the bending moment is applied. Similarly, F_{sp} is the applied compressive force, calculated via Equation (4), and A_d is the total bedded area.

$$M_{sp} = 9.81m_2 \bullet \left(d_2 - \frac{t_u}{2}\right) + 9.81m_1 \bullet \left(d_1 - \frac{t_u}{2}\right) \tag{3}$$

$$F_{sp} = 9.81 \bullet (m_1 + m_2 + m_3) \tag{4}$$

Load applied to the specimen, m_2, is applied by the individual performing the test either through their own body mass or through the application of weights. This force must be applied at an even rate to avoid dynamic load effects until failure of the joint is achieved.

3.2. Triplet shear test – Shear bond strength

The shear bond strength of each masonry combination was examined through the application of the unconfined triplet shear test as specified by EN1052-3 [7]. Each test specimen consisted of three masonry units bonded together with two mortar joints. These triplets were then

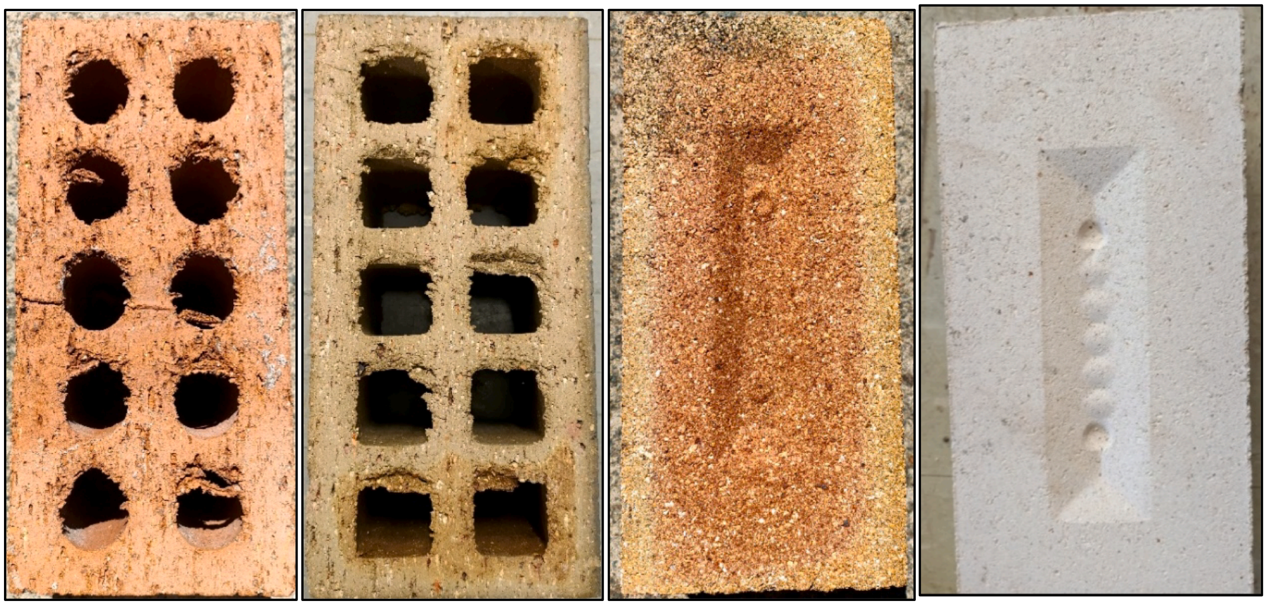

(a) (b) (c) (d)

Fig. 4. Selected masonry units. Extruded units (a) Type 1 and (b) Type 2. Pressed units (c) Type 1 and (d) Type 2.

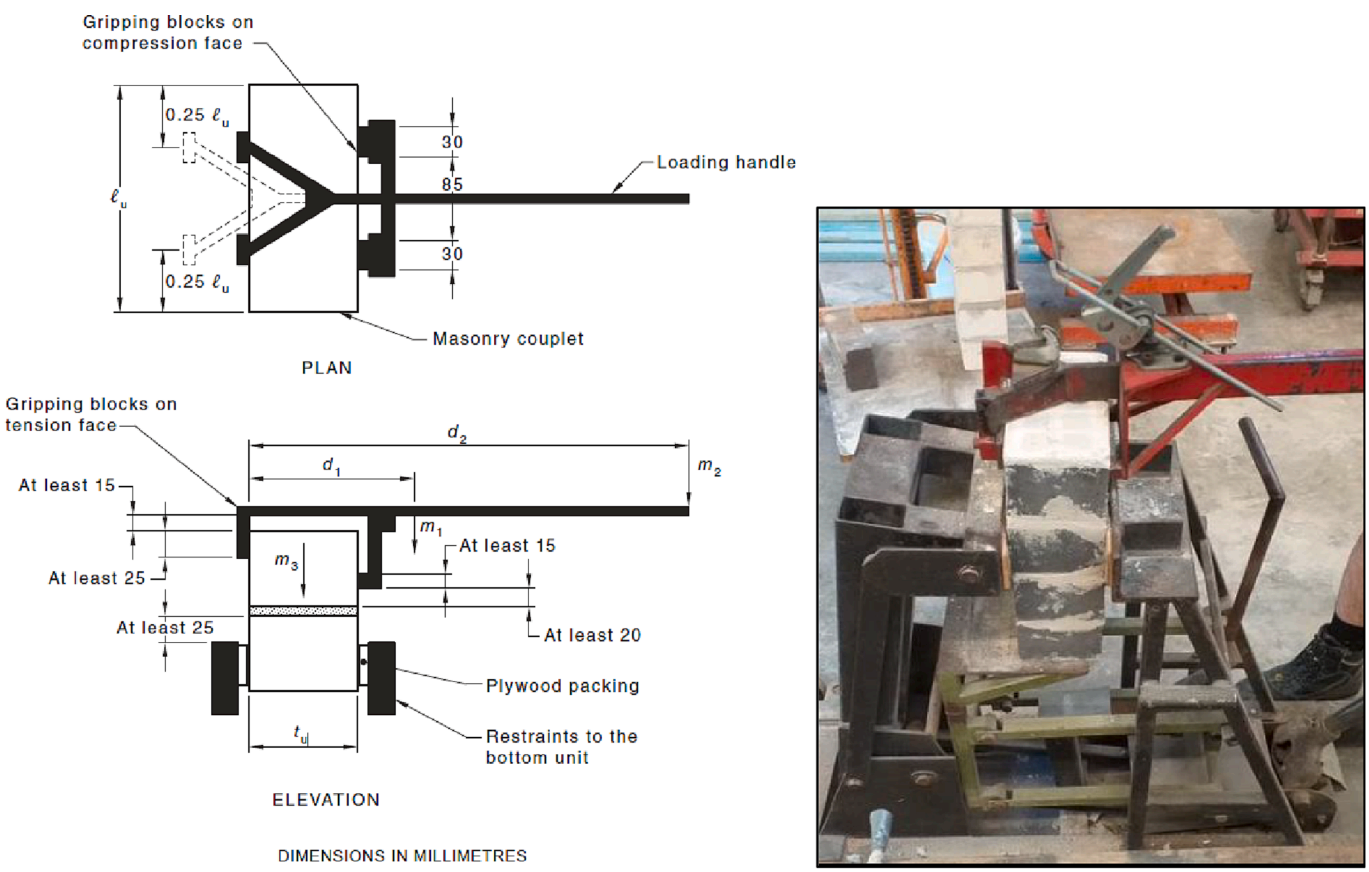

Fig. 5. Schematic diagram and test set-up of the bond wrench set-up [30].

subjected to a load applied to the central unit, parallel to the longitudinal direction of the mortar joints. The triplet was restrained via plate-stiffened roller supports at the base of the specimen, adjacent to the outside edges of the loaded mortar joints. A schematic of the laboratory set-up is shown in Fig. 6.

The maximum applied force required to fail the triplet, $F_{i,max}$, is recorded and the shear strength of the specimen calculated from Equation (5). In the case of an unconfined triplet shear test, as was utilised in this study, estimates of shear strength represent the shear bond strength only.

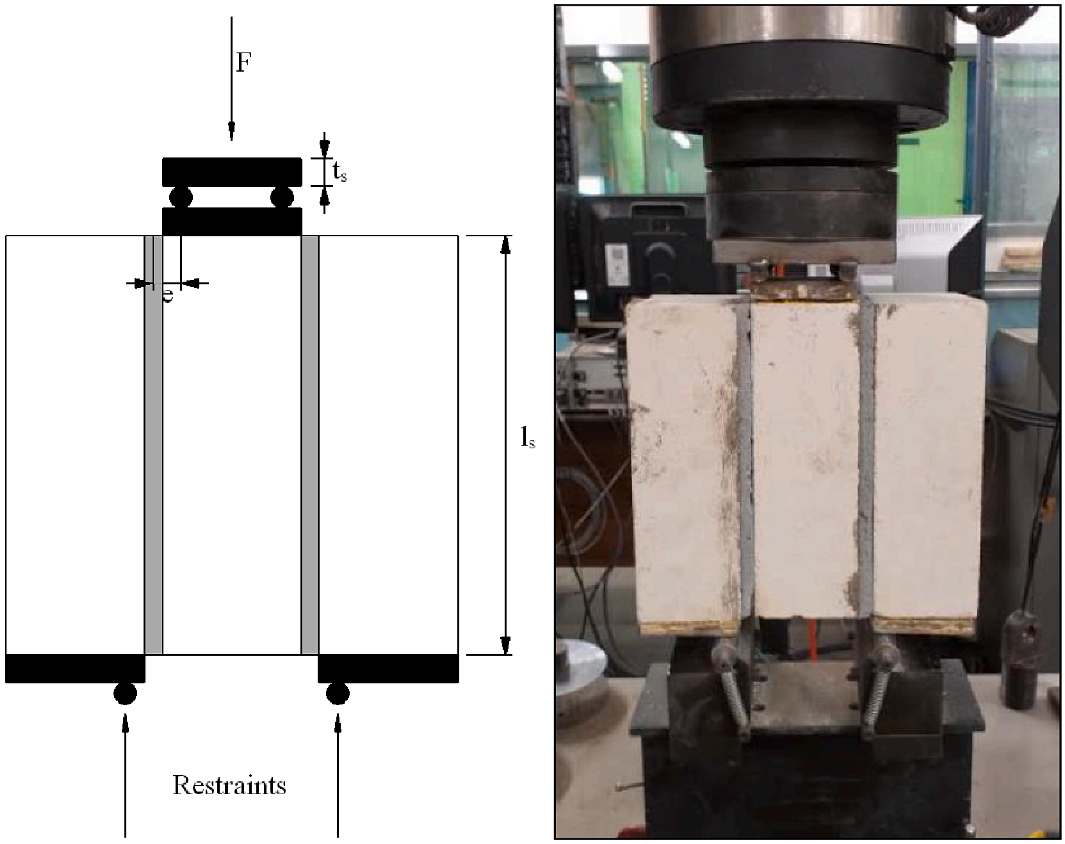

Fig. 6. Schematic diagram and test set-up of the triplet shear test. Adapted from EN1052-3 [7].

$$f_{voi} = \frac{F_{i,max}}{2A_i} \tag{5}$$

where A_i is the full bedded area of the masonry units. As with the bond wrench test, load is applied gradually to the specimen until failure is achieved. This was done through the use of an Instron Universal Testing System. Displacement was applied at a constant rate of 1 mm per minute, resulting in the vertical reaction force shown in Fig. 6.

As noted in Section 2.3, previous studies of masonry behaviour under shear loading indicate that several correction factors should be considered in estimates of shear bond strength performed in accordance with EN1052-3 [7]. Riddington et al., [22] determined through the use of finite element modelling that, during an unconfined triplet shear test, the distribution of stresses is sufficiently non-uniform that the true shear bond strength is as much as 50% greater than the simple estimate of shear strength determined from Equation (5). Furthermore, the work of Lawrence [13] on a wide range of triplet shear tests indicates that, due the presence of two potential failure planes, the mean joint shear strength is 1.14 times greater than the triplet shear strength as the weaker of the two interfaces shall always fail first. This conclusion is based upon a coefficient of variation (COV: defined as the mean divided by the standard deviation) of shear bond strength of 21%, the mean COV observed in the Lawrence's study.

Considering these two factors in this study's estimates of shear bond strength results in a correction factor of 1.71 to be applied to the values of f_{voi}.

3.3. Modulus of rupture test – flexural tensile unit strength

In order to estimate the flexural tensile strength of masonry units, the lateral modulus of rupture test outlined by AS/NZS 4456.15 [26] was employed. This test is a four-point beam bending test applied to a specimen of three masonry units bonded lengthwise using a high strength epoxy resin. This resin, Selleys' Super Strength Araldite, is of a sufficiently high strength (up to 15 MPa, after [24]) to produce a thin interface that is stronger than the tensile strength of the units under investigation. A schematic of the test set-up is presented in Fig. 7.

The unit orientation shown in Fig. 7's test set-up is most relevant to URM walls subjected to out-of-plane bending, such as is induced by wind- or seismic-events. Shallow URM beams, such as lintels, may be subjected to a similar loading action at an orientation of 90° to that shown in Fig. 7. However, this application of masonry is uncommon, and typically avoided in masonry construction due to URM's poor tensile performance. Furthermore, while this alternative orientation may be relevant to the behaviour of URM shear walls, such structures are usually sufficiently deep to ensure that, locally, units are subject to either tension or compression, rather than flexural action.

In addition to the points above, no consideration has been given to the effects of a smooth or rough finish on the stretcher face of the tested units. A visual inspection of the units shown in Fig. 4 indicates that neither stretcher face is significantly smoother. Furthermore, an exhaustive study of alternative orientations of modulus of rupture specimens to accommodate the effects of surface roughness, as well as the loading mechanisms discussed above, has been deemed outside the scope of this study.

The maximum load, W, required to induce failure is recorded and lateral modulus of rupture, f_{ut}, is estimated from Equation (6).

$$f_{ut} = \frac{M}{Z} \tag{6}$$

where M is the maximum recorded bending moment, calculated from Equation (7), and Z is either the net or gross section modulus of the specimen. While AS/NZS 4456-15 [26] recommends that no allowance be made in the calculation of section modulus for any reductions in the cross-section of the specimen from frogs or perforations, the effect of

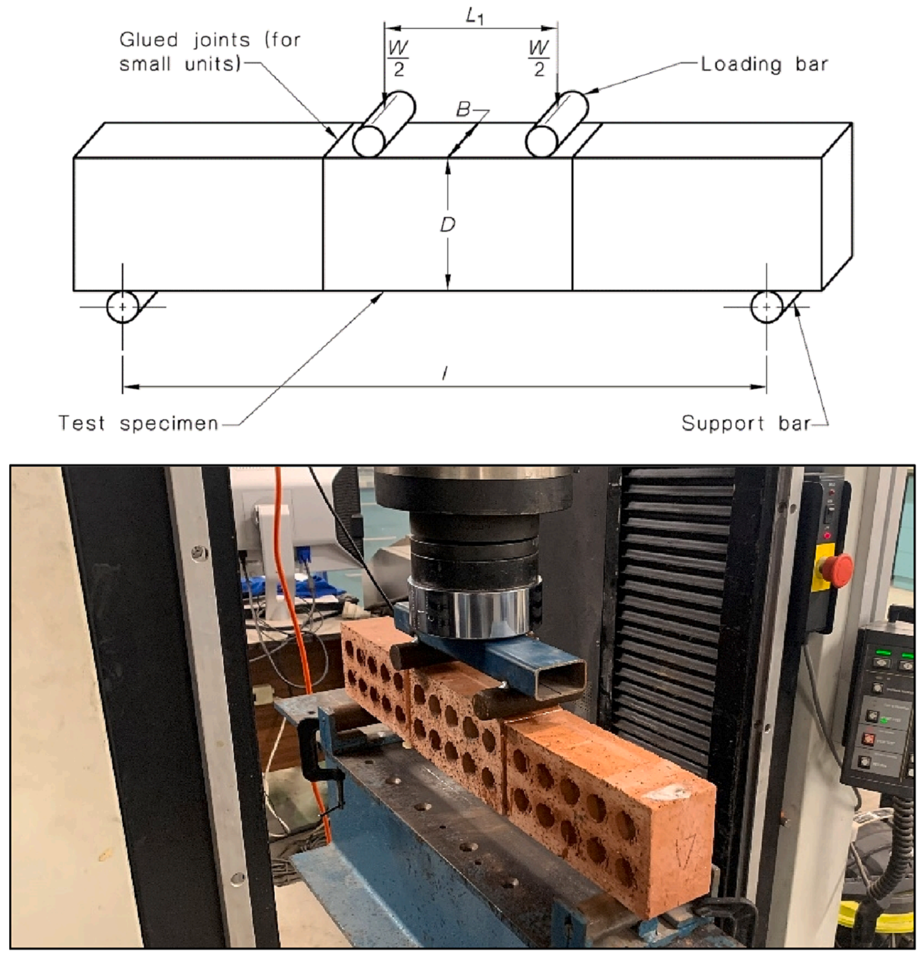

Fig. 7. Schematic diagram and test set-up of the modulus of rupture test [26].

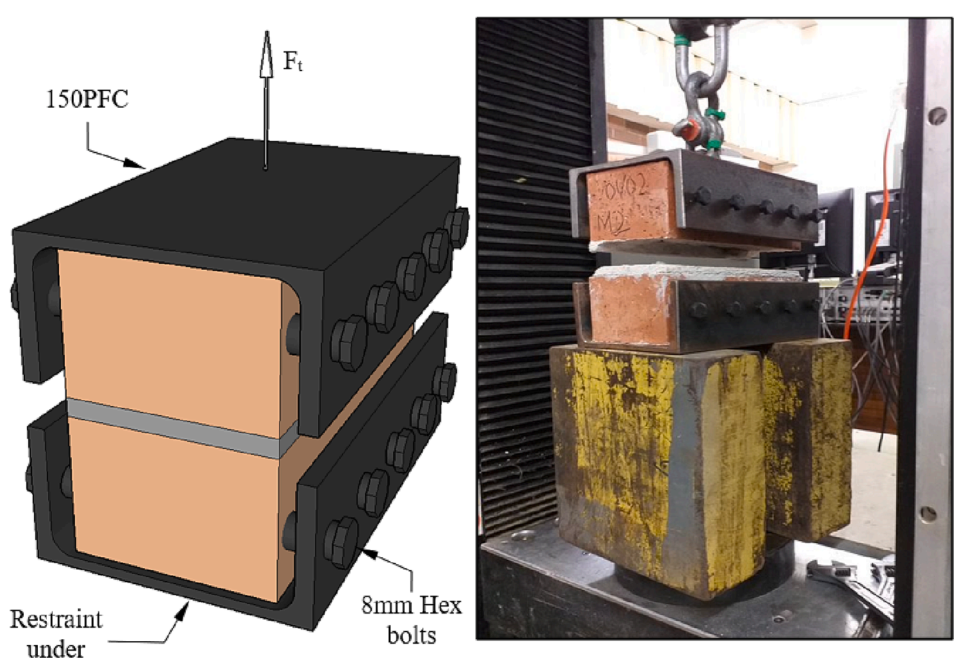

Fig. 8. Isometric and as-constructed image of apparatus for direct tension on unit-mortar interface; image captured after failure of joint.

considering net section is discussed in Section 4.2.

$$M = W\left(\frac{l - l_1}{4}\right) \tag{7}$$

Similar to the triplet shear test, specimens were tested in an Instron Universal Testing System with a reactionary load applied from a vertical displacement, maintained at a constant rate of 1 mm per minute so as to mitigate dynamic load effects.

3.4. Couplet tension test – direct tensile bond strength

The first of the two non-standard testing methods devised in this study is the couplet tension test used to estimate the direct tensile bond strength of the unit-mortar interface. Specimens for this test consisted of two masonry units bonded with a single mortar joint to form a couplet. Both the top and bottom units were clamped into a 150PFC (parallel flanged channel section) with five 8 mm hex head bolts on both longitudinal faces of both channels. A displacement controlled tensile strain was then applied to the top channel at a constant rate of 1 mm per minute, as in the previous tests. A vertical restraint was mirrored on the bottom channel consisting of a chain attached to the base of the Instron Universal Testing System. This restraint provided a vertical reaction against the tensile loading. As may be seen in Fig. 8, two timber blocks were placed under each specimen. These were utilised in order to support the specimen prior to the application of any load, as well as to prevent the bottom half of a failed specimen from falling and breaking further, obscuring the failure pattern of the joint. This was necessary due to the tension-only nature of the restraint system.

Once the weight of the unit was supported by the testing apparatus, further tensile loading was applied until failure was achieved. The complete load–displacement behaviour of each test was recorded, along with the mass of the unit to calculate an accurate peak tensile load. The load–displacement behaviour in these tests was not sufficiently accurate past the point of peak loading to facilitate an investigation into strain softening or fracture energy as in similar investigations of the tensile behaviour of masonry [35]. Estimates of tensile strength were made by simply dividing the maximum recorded tensile load by the total bedded area of the couplet, similar to the simplified beam theory recommended for the bond wrench test outlined in Section 3.1.

When securing each specimen, the tightening of bolts was performed carefully and uniformly so as to ensure a firm and consistent restraint across the length of the specimen while ensuring that bolts were not over tensioned resulting in crushing or local weakening of the specimen at bolt locations. The use of bolts introduced a limitation in the testing method as an insufficient amount of tension would result in slipping prior to failure, requiring the test to be disregarded. Conversely, over tensioning of bolts could result in the edge-blowout of low strength units or hairline fractures through the cross-section of the unit, as shown in Fig. 9. It was noted that in most cases of these hairline fractures, splitting of the units typically did not occur during testing and a suitable estimate of tensile strength could be achieved.

3.5. Unit direct tension test – direct tensile unit strength

Finally, the direct tensile strength of masonry units was estimated through the application of a direct tension test devised for this study. The specimens for this test consisted of a single masonry unit with a steel plate (76 mm × 110 mm × 10 mm) bonded to either end of the unit with the same high strength adhesive used for the modulus of rupture tests. Each plate was affixed with a steel chain, attached to the specimen via a welded lifting lug. The top chain was utilised to apply a tensile load, while the bottom provided a vertical restraint via another lifting lug attached to the Intron testing system. An isometric and as-constructed image of the testing apparatus is shown in Fig. 10.

Unlike the couplet tension test, the absence of tensioned bolts removed the risk associated with local crushing or hairline fracturing of the tested specimens. However, a key concern with the adopted testing method was that a poor bond between the steel and masonry, or local weakening of the ends of the specimens during preparation, would invalidate the results of the test. In cases where local spalling at the interface between steel and masonry, or a direct failure of the epoxy instead of the unit, was observed, these test results were disregarded, and another specimen was prepared.

A tensile strain was applied to all specimens via a constant vertical displacement, maintained at a rate of 1 mm per minute, as in previous tests, to mitigate dynamic effects. As with the couplet tests, the tensile strength of the masonry units was estimated by dividing the maximum recorded load by the cross-sectional area of the units, and consideration of the net section of the specimens was made, as discussed in Section 4.2. Furthermore, no investigation into effects such as strain softening or fracture energy was performed due to the limited post-peak, load–displacement data available, as in the case of the direct tensile tests of mortar joints.

4. Results and discussion

The experimental results of this study, presented below, allow for relationships to be estimated between the direct and flexural tensile bond strengths, the flexural tensile and shear bond strengths, and the direct and flexural tensile strengths of masonry units. These

Fig. 9. Examples of unit splitting during or after testing due to over-tensioning of bolts.

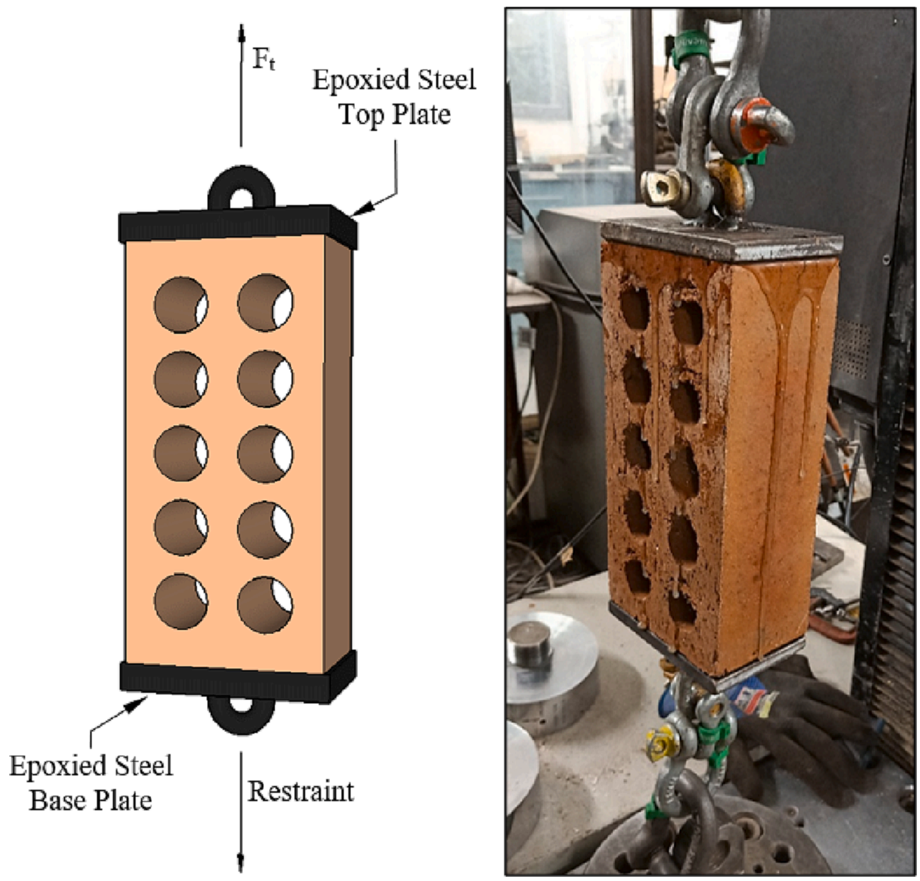

Fig. 10. Isometric and as-constructed image of apparatus for direct tension testing of masonry units.

Table 2
Measured mean and characteristic flexural tensile and direct tensile bond strengths with comparisons of these properties.

Unit	Mort-ar[1]	Flexural tensile bond strength AS3700				Direct tensile bond strength				Comparison	
		(1) Mean (MPa) [COV]	(2) f'_{mt} (MPa) COV = 30%	(3) f'_{mt} (MPa) Calc. COV	(4) Sample size	(5) Mean (MPa) [COV]	(6) f'_t (MPa) COV = 30%	(7) f'_t (MPa) Calc. COV	(8) Sample size	(9) $\frac{(1)}{(5)}$	(10) $\frac{(3)}{(7)}$
Ext. clay brick 1	1	0.221 [17%]	0.111	0.140	5	0.097 [11%]	0.043	0.068	3	2.27	2.06
	2	0.315 [37%]	0.135	0.120	5	0.128 [17%]	0.066	0.083	5	2.46	1.45
	3	0.554 [12%]	0.289	0.393	5	0.154 [22%]	0.067	0.076	5	3.61	5.16
	4	0.502 [19%]	0.254	0.307	5	0.318 [17%]	0.158	0.196	5	1.58	1.57
	5	0.231 [39%]	0.052	0.045	5	0.091 [49%]	0.022	0.016	5	2.55	2.77
	7	0.480 [17%]	0.243	0.303	5	0.227 [52%]	0.043	0.031	5	2.12	9.82
Ext. clay brick 2	1	0.221 [7.5%]	0.125	0.184	4	0.093 [12%]	0.049	0.067	5	2.37	2.76
	2	0.308 [10%]	0.160	0.224	5	0.101 [22%]	0.041	0.046	5	3.06	4.83
	3	0.732 [17%]	0.337	0.420	5	0.239 [21%]	0.115	0.133	5	3.07	3.17
	4	0.437 [26%]	0.176	0.189	5	0.281 [24%]	0.121	0.135	5	1.55	1.39
	5	0.232 [13%]	0.119	0.158	5	0.114 [21%]	0.045	0.053	5	2.03	3.01
	7	0.585 [30%]	0.262	0.260	5	0.337 [17%]	0.175	0.220	5	1.73	1.18
Press-ed clay brick 1[2]	1	0.178 [53%]	0.053	0.036	5	0.116 [26%]	0.040	0.042	5	1.53	0.85
	2	0.360 [35%]	0.140	0.130	5	0.163 [19%]	0.065	0.077	5	2.21	1.67
	4	0.598 [21%]	0.249	0.291	5	0.341 [11%]	0.181	0.249	5	1.75	1.17
	5	0.684 [20%]	0.300	0.354	5	0.286 [25%]	0.122	0.134	5	2.39	2.65
	7	0.648 [19%]	0.327	0.396	5	0.455 [13%]	0.232	0.308	5	1.42	1.29
Press-ed clay brick 2[2]	1	0.243 [21%]	0.106	0.125	5	0.109 [7.2%]	0.060	0.088	5	2.24	1.42
	2	0.165 [24%]	0.078	0.086	5	0.105 [32%]	0.041	0.039	5	1.57	2.18
	4	0.447 [24%]	0.214	0.236	5	0.285 [14%]	0.143	0.186	5	1.57	1.27
	5	0.238 [67%]	0.039	0.025	3	0.238 [23%]	0.092	0.105	5	1.00	0.24
	7	0.392 [26%]	0.175	0.188	5	0.327 [16%]	0.148	0.202	4	1.20	0.93
									Mean	**2.06**	**2.40**
									COV	**31.5%**	**85.8%**

[1] Mortar mix 6 was not utilised in these tests.
[2] Mortar mix 3 with noted units was excluded due to clear outliers in results.

relationships may be applied to future numerical modelling of masonry structures, as well as informing analytical models of masonry behaviour, such as a suitable bond strength to be assumed for a mortar joint subjected to pure tensile loading.

In the subsequent sections, determination of the characteristic values for the flexural tensile and direct tensile strengths of both the masonry units and the unit-mortar interface was determined in accordance with AS 3700 [30], see Equations (8) and (9) where k_k is the characteristic value factor derived from AS 3700, f_{spl} is the least of the individual test results, and f_{ksp} is the lower 5th percentile value for the set of test results.

$$f' = k_k f_{spl} \text{ for } n < 10 \tag{8}$$

$$f' = k_k f_{ksp} \text{ for } n \geq 10 \tag{9}$$

The characteristic values for shear bond strength were calculated as per the above methodology, as well as the statistical method outlined in EN1052-3, see Equation (10), where Y_c is calculated as per Equation (11), Y_{mean} is the average value of the $\log_{10}$ of the initial shear strength values, k is the characteristic value factor derived from EN1052-3, and s is the standard deviation of the n log values.

$$f_{vko} = \text{antilog}_{10} Y_c \tag{10}$$

$$Y_c = Y_{mean} - k \times s \tag{11}$$

In examining the statistical properties of these relationships, consideration of the COV must be made. In order to accurately estimate the variability of the subsequently discussed relationships, the calculated COV must be adjusted to consider the effects of variability in the testing procedure and in the specimens themselves [6]. The accuracy of the testing procedures outlined in Section 3 for example are dependent upon the placement of each experimental apparatus, the skill of the individual operator [33] and the accuracy of recording equipment. However, as each of the datapoints presented in Tables 2 and 4 are typically an average of 4 or 5 individual measurements, or 19 or 20 in the case of Table 3, it is reasonable to assume that most of this experimental variability is factored out. This assumption will result in a slight overestimation of the variability of the relationship between each of these material properties, and is consistent with the statistical analyses of other materials such as concrete and its reinforcement [33].

4.1. Direct and flexural tensile bond strengths

The ratio between the flexural and direct tensile bond strengths was assessed through the examination of mean strength values, using all mortar mixes noted in Table 1, except for mix 6, in combination with the four masonry unit types presented in Fig. 4. A mean value of the ratio of flexural and direct tensile bond strengths of 2.06 was estimated with a COV equal to 31.5%. This estimated mean ratio, as well as a similar ratio presented by Riddington and Jukes [23] and the AS 3600 [27] ratio for plain concrete, is shown against the recorded experimental data in Fig. 11. Further to this, a mean ratio of 2.40 with a notably higher COV of 85.8% was estimated from the characteristic strengths of both properties, estimated in accordance with AS3700 [30]. This increase in COV is not unexpected as the notably different COVs for individual data points were observed, resulting in more variable characteristic strengths.

For each of the specimen types presented in Table 2, a sample size of five mortar joints was initially constructed. In some cases, a sample size of only three or four data points has been noted, due to either joints failing prior to testing or as a result of an invalid test, as defined by AS 3700 [30]. The individual sample sizes in this study are limited by the large number of masonry configurations that have been examined.

It should also be noted that the application of the bond wrench test yielded high variability for some specimen types, resulting in the large error bars shown in Fig. 11. Furthermore, combinations of mortar mix 3 with either of the pressed clay units were excluded from the results due to the exceptionally high errors and outlying results.

While the calculated ratio of 2.06 is significantly more conservative than the ratio of 1.50 or 1.67 inferred from AS 3600 [27,29] for the design of plain concrete, or the 1.50 reported for masonry presented by Van der Pluijm [35], it is not inconsistent with the findings of Riddington and Jukes [23] who estimated a similar ratio of 1.9 based upon the differing distribution of stresses estimated numerically.

In addition to Fig. 11, the complete set of measured results, including the mean and characteristic values of each individual unit-mortar combination, are presented in Table 2. These results highlight those unit and mortar combinations whose measured properties were more variable, as well as presenting estimations of the characteristic properties calculated both in accordance with COV recommended by AS 3700 [30], and the measured variability. It should be noted that while several of the error bars displayed in Fig. 11 appear to be quite large, few sets of flexural tensile bond strength exhibited a variability inconsistent with that noted in the current Australian Standard [30].

Finally, the sensitivity of the estimated ratio to changes in flexural tensile strength was examined. This sensitivity is an important consideration as a high dependence upon the flexural tensile strength would indicate that the estimated ratio is only relevant over a small range of tensile strength. Furthermore, this would indicate that a simple linear relationship between the two properties is an inaccurate description. The results of this analysis are presented in Fig. 12. It can be observed that a linear model of the dependence of the ratio between tensile bond strengths on the flexural tensile bond strength has a coefficient of determination of only 0.03, indicating that changes in the bond strength have almost no effect on the estimated ratio.

4.2. Direct and flexural tensile unit strengths

As with the bond strength of the unit-mortar interface, the current study examined the relationship between the flexural tensile and direct tensile strengths of fired clay, masonry units. However, in this case, a small sample size of only three types of units was used. Future studies are planned to expand upon the findings presented in this section. In addition, while the examination of the unit-mortar interface utilised sets

Table 3
Measured mean and characteristic flexural tensile and direct tensile strengths of masonry units with comparisons of these properties.

Unit[1]	Flexural tensile strength			Direct tensile strength			Comparison	
	(1) Mean (MPa) [COV]	(2) f'_{ut} (MPa) Est. COV	(3) Sample size	(4) Mean (MPa) [COV]	(5) f'_{bt} (MPa) Est. COV	(6) Sample size	(7) $\frac{(1)}{(4)}$	(8) $\frac{(2)}{(5)}$
Ext. clay brick 1	2.54 [44%]	0.34	20	1.98 [28%]	0.74	20	1.28	0.46
Ext. clay brick 2	2.70 [29%]	1.37	20	2.43 [33%]	0.62	20	1.11	2.2
Pressed clay brick 2	0.98 [39%]	0.21	19	0.66 [25%]	0.28	20	1.49	0.76
						Average	**1.29**	**1.14**
						COV	**14.7%**	**81.6%**

[1] All results are derived considering the net section properties.
[2]Pressed clay brick 1 was not utilised in these tests.

Table 4
Measured mean and characteristic flexural tensile and shear bond strengths, with comparisons of these properties.

Unit	Mortar	Flexural tensile bond strength AS3700				Shear bond strength EN1052-3				Comparison	
		(1) Mean (MPa) [COV]	(2) f'_{mt} (MPa) COV = 30%	(3) f'_{mt} (MPa) Calc. COV	(4) Sample Size	(5) Mean (MPa) [COV]	(6) EN Statistical f_{vko} (MPa)	(7) AS3700 Characteristic (MPa) Calc. COV	(8) Sample size	(9) $\frac{(5)}{(1)}$	(10) $\frac{(6)}{(3)}$
Ext. clay brick 1	1	0.330 [12%]	0.175	0.236	5	0.480 [17%]	0.319	0.340	4	1.46	1.35
	2	0.517 [33%]	0.205	0.197	5	0.820 [14%]	0.604	0.648	5	1.59	3.07
	3	0.834 [23%]	0.373	0.417	5	1.198 [21%]	0.734	0.840	5	1.44	1.76
	4	0.621 [17%]	0.295	0.368	5	0.986 [18%]	0.648	0.726	5	1.59	1.76
	5	0.920 [10%]	0.500	0.701	5	1.266 [35%]	0.533	0.703	5	1.38	0.76
	6	1.078 [24%]	0.479	0.530	5	1.808 [15%]	1.265	1.391	5	1.68	2.39
	7	0.461 [20%]	0.190	0.225	5	0.760 [16%]	0.532	0.579	5	1.65	2.37
Ext. clay brick 2	1	0.374 [9%]	0.183	0.281	5	0.675 [23%]	0.369	0.459	5	1.81	0.96
	2	0.903 [14%]	0.422	0.554	5	1.145 [11%]	0.874	0.942	5	1.27	1.55
	3	1.420 [21%]	0.556	0.652	5	1.365 [33%]	0.65	0.784	5	0.96	1.59
	4	0.536 [17%]	0.276	0.345	5	0.835 [20%]	0.491	0.598	5	1.56	3.01
	5	1.194 [35%]	0.443	0.411	5	1.369 [26%]	0.722	0.883	5	1.15	0.08
	6	0.973 [15%]	0.435	0.565	5	1.400 [18%]	0.922	1.038	5	1.44	2.75
	7	0.347 [18%]	0.162	0.200	4	0.629 [15%]	0.435	0.484	5	1.81	1.31
Pressed clay brick 1[1]	1	0.486 [16%]	0.241	0.309	5	0.399 [13%]	0.295	0.320	5	0.82	1.58
	2	0.871 [23%]	0.383	0.429	5	0.812 [9%]	0.665	0.699	5	0.93	1.00
	4	0.782 [15%]	0.383	0.498	5	1.082 [14%]	0.792	0.857	5	1.38	1.42
	5	0.784 [48%]	0.283	0.212	5	1.037 [23%]	0.638	0.703	5	1.32	1.75
	6	1.620 [13%]	0.760	1.007	5	0.974 [65%]	0.082	0.419	5	0.60	1.63
	7	0.532 [21%]	0.241	0.280	5	1.003 [11%]	0.772	0.826	5	1.88	2.18
Pressed clay brick 2[1]	1	0.229 [35%]	0.067	0.062	5	0.298 [22%]	0.172	0.205	5	1.30	2.78
	2	0.304 [40%]	0.087	0.075	5	0.275 [31%]	0.115	0.162	5	0.90	1.54
	4	0.379 [13%]	0.179	0.239	5	0.548 [27%]	0.293	0.35	5	1.44	1.23
	5	0.241 [51%]	0.060	0.043	5	0.452 [29%]	0.231	0.276	5	1.87	5.35
	6	0.587 [56%]	0.119	0.081	4	0.270 [18%]	0.173	0.197	5	0.46	2.15
	7	0.528 [21%]	0.232	0.268	5	0.609 [11%]	0.477	0.507	5	1.15	1.78
									Mean	**1.34**	**1.89**
									COV	**28.4%**	**52.8%**

[1] Mortar mix 3 with noted units was excluded to due clear outliers in results.

of up to five individual specimens of each unit-mortar combination, investigation into the behaviour of masonry units was done in sets of 20. This was done to offset the limited number of unit types and was facilitated by the speed with which tests could be performed without the need to batch and cure mortar.

Considering the net sections of the examined clay bricks, a mean ratio between the flexural tensile and direct tensile strengths of 1.29 was estimated, with a reasonably small COV of 14.7%. Furthermore, a ratio of 1.14, with a significantly larger COV of 81.6%, was determined for the characteristic values of both tensile strengths. This increased variability is consistent with the results presented for the unit-mortar interface and have been exacerbated by the larger COV of the material properties and smaller number of unit types. The complete set of experimental results is presented in Table 3.

It has been noted that the above material properties have been estimated using the net section properties of the clay brick units, taking into account the perforation pattern of extruded units and frog geometry of the pressed units (see Section 3 for a detailed breakdown of these geometric properties), as well as the failure pattern of each individual specimen. This is inconsistent with the method outlined in AS/NZS 4456.15 [26], which conservatively specifies that the gross section properties be utilised. However, given the differing section properties of

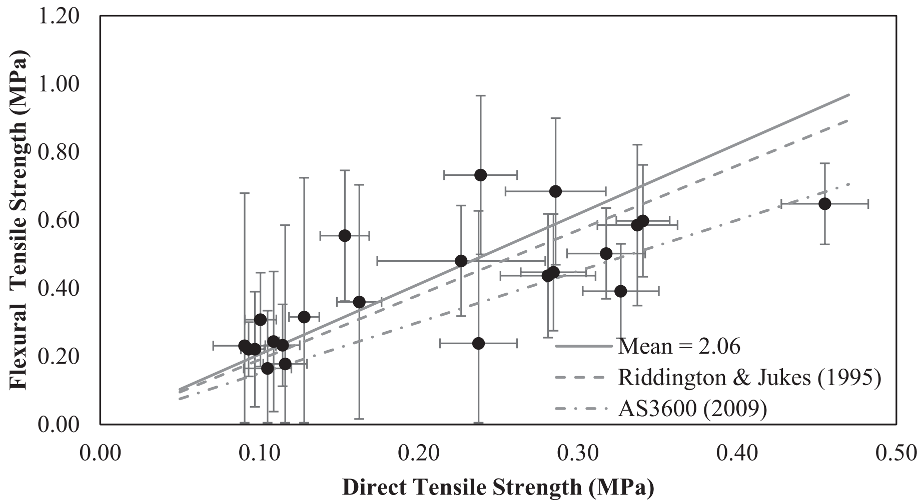

Fig. 11. Comparison of mean flexural and mean direct tensile bond strengths estimated for clay brick masonry with standard error bars shown. The experimentally estimated mean ratio of 2.06 and literary estimates of the same [23;27] are noted.

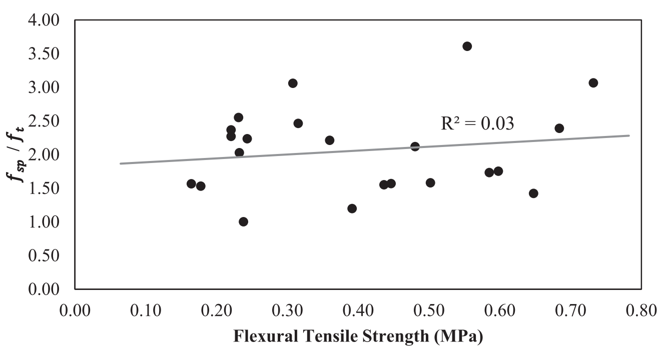

Fig. 12. Comparison between the mean flexural tensile bond strength and ratio between flexural and direct bond strengths.

each type of unit, failure to account for the net section will yield results not representative of the true relationship between these material properties, but rather a value that is a function of both the material and the geometry of the selected units.

Furthermore, for the extruded units considered in this study, the presence of core holes reduces the net area significantly more than it does the net section modulus, as a result, considering only the gross section will cause the direct tensile strength to be underestimated more than the flexural tensile strength.

However, accounting for the net section properties of each unit introduces a limitation in some applications of the results presented in this section. FE modelling of masonry structures typically does not account for perforations or other reduction in section size. As a result, a ratio accurately relating the tensile strengths of units considering their gross section properties is also needed to accurately model equivalent solid finite elements of masonry units.

In such applications, it is recommended that the ratio between flexural tensile and direct tensile unit strengths first be determined using the net section of the unit, as described in Table 3. This ratio should then be corrected by multiplying by a shape factor, representative of the ratio between the gross and net section moduli and cross-sectional areas. The resultant correction factor would then produce an estimate of the ratio between flexural tensile and direct tensile unit strengths based on the gross section properties for an arbitrary geometric configuration.

This shape factor is a function of the gross and net section moduli and cross-sectional areas of the unit under examination. Note that Equation (12) is relevant for the conversion of a net direct tensile strength to a gross direct tensile strength. The inverse of this expression may be used in a similar estimation of the gross flexural tensile strength as a function of a measured direct tensile strength.

$$\lambda_{shape} = \left(\frac{Z_{net}}{Z_{gross}}\right) \times \left(\frac{A_{gross}}{A_{net}}\right) \tag{12}$$

4.2.1. *Effects of anisotropy on stress-concentrations*

In considering the net cross-section of a masonry unit subjected to either direct or flexural tensile strength, a simplifying assumption made by the shape factor presented in Equation (12) is that tensile stresses will remain either uniform (direct tension) or linearly variable with a constant slope (flexural tension) irrespective of the type of perforations present in the masonry. This simplification ignores the anisotropy of most masonry units, extruded (cored) units in particular.

In a direct tensile test, failure will almost exclusively initiate through the largest perforations in extruded masonry units due to their effect on the net cross-sectional area. However, the shape of these perforations

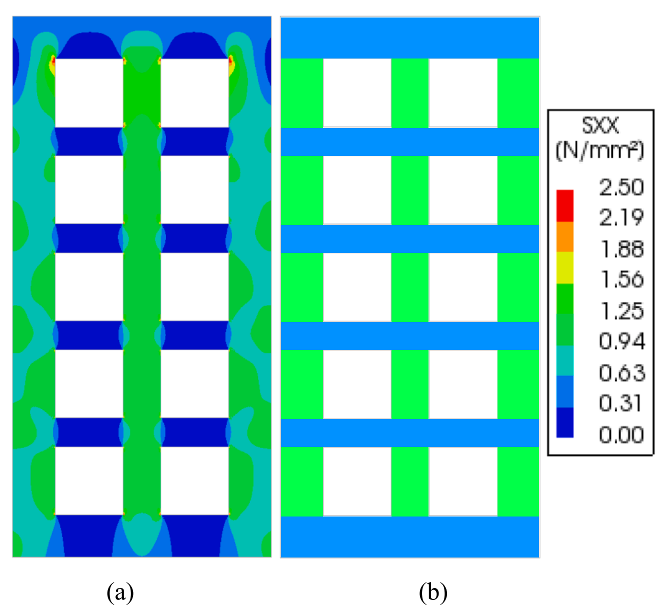

Fig. 13. Effect of stress concentrations in extruded masonry unit subject to direct tensile loading. (a) Stress concentrations considered. (b) Stress concentrations ignored.

can lead to stress concentrations which will initiate failure at a lower applied tensile load. This can be observed in the FEA results presented in Fig. 13.

Preliminary FE modelling indicates that, for the extruded masonry utilised in this study, points of stress concentration under direct tensile loading may be 2 to 2.5 times higher than the value estimated by simple consideration of the net section. Similarly, a stress concentration of approximately 1.35 times the value determined from the net section properties may be observed under flexural tensile loading. These FEA results are presented in Fig. 14. The values of S_{XX} presented in this figure, as well as in Fig. 13, reflect the stress concentration factor, i.e.: the proportional increase in tensile stress relative to the value determined without consideration of stress concentrations.

Given the small sample size for masonry unit behaviour presented in this study, and the complexity of analysis required to adequately quantify the effects of stress concentrations for a wide range of perforation patterns, these effects are considered outside the scope of this study. However, unit geometry and anisotropy should be considered prior to the application of the findings presented in Table 3.

4.3. Flexural tensile and shear bond strengths

Similar to the examination of tensile bond strengths, the relationship between the flexural tensile and shear bond strengths was assessed using mean strength values estimated from unit-mortar combination of all mortar mixes noted in Table 1, and all masonry units shown in Fig. 4. A mean ratio for shear bond strength divided by flexural tensile bond strength of 1.34 was estimated with a COV of 28.4%. Further to this, a ratio between the characteristic strengths was estimated as 1.89 with a COV of 52.8%. While the mean ratio is not inconsistent with the current code relationship of $f'_{ms} = 1.25 f'_{mt}$, as well as the value of 1.19 determined by Masia et al., [16], the ratio of characteristic strengths is notably larger than the AS3700 [30] recommendation. It should be noted that while the characteristic flexural tensile bond strength was estimated in accordance with AS3700 [30], the characteristic shear bond strength used in this analysis was calculated using the statistical method presented in EN1052-3 [7] as the use of a lognormal distribution of shear bond strengths has been shown in literature to more accurately represent their statistical variation [13].

In addition to the estimation of this mean strength ratio, the correlation between these two properties was investigated. It is not unreasonable to assume that a high degree of correlation exists between the tensile and shear bond strengths as either a poor- or high-quality joint will result in correspondingly low or high tensile and shear bond strengths. However, the assumption of a full correlation between these two properties such that an increase in the assumed tensile strength of a model results in a proportionally equivalent increase in shear strength may be unreasonable. Furthermore, the assumption of a full correlation can limit the results of a statistical analysis of URM structures. For example, a high tensile strength, but low shear strength may result in the less favourable shear failure modes for a masonry shear wall. While simply assuming the properties are fully correlated, as recommended by AS 3700 [30], may limit a model's outcome to the more favourable flexural rocking modes, resulting in an unconservative estimate of the ductility of the structure. As such, it is important to accurately quantify the correlation coefficient between these two properties when performing a stochastic masonry analysis.

From the current study, a correlation coefficient of 0.75 was calculated for the clay brick masonry combinations presented in Table 4. This value indicates that a strong correlation exists between the two

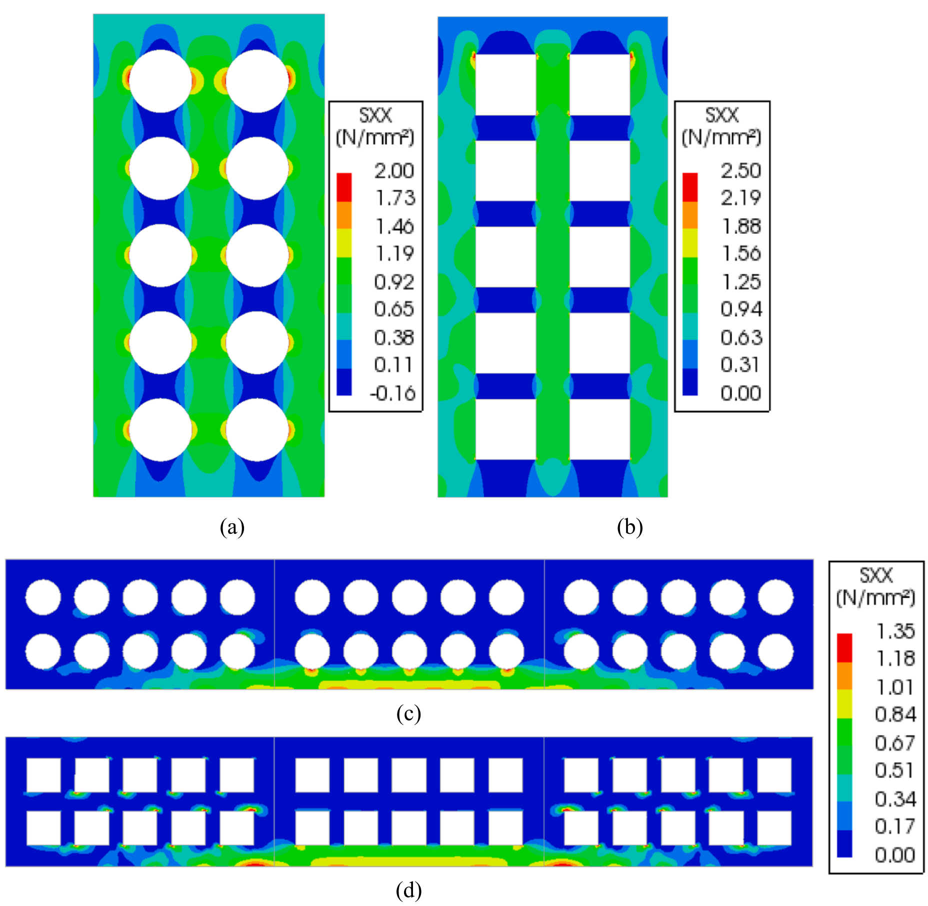

Fig. 14. Relative stress concentrations in extruded masonry under direct tensile loading for units (a) Type 1 and (b) Type 2, and flexure for units (c) Type 1 and (d) Type 2.

parameters, but not a full correlation, reinforcing the previous assertion regarding limitations in simplified stochastic models. In addition, a correlation coefficient of 0.89 was found through an analysis of the experimental results of Masia et al., [16]. While the results of this study do not contradict those of Masia et al., this previous study considered both clay brick and concrete block masonry units. As such, further study into the correlation of the shear and tensile properties of concrete blockwork masonry is recommended.

The ratio between shear and flexural tensile bond strengths determined in this study, along with the ratio determined from the results of Masia et al., is presented in Fig. 15 against the individual mean strengths of each masonry combination.

Shown in Table 4 is the complete set of experimental results. These results present the measured variabilities in the bond wrench tests and are observed to be not dissimilar to those shown in Table 2. Furthermore, while EN1052-3 [7] does not provide a standardised value of the COV of shear bond strength, those values presented in Table 4 are not inconsistent with previous statistical studies of shear bond strength [9,14].

The sensitivity of the estimated ratio of shear and flexural bond strengths to changes in flexural tensile bond strength has also been assessed. In this case, the flexural tensile bond strength was adopted as the governing material parameter so as to be consistent with the formula presented in AS 3700 [30] (see Equation (1)). As may be seen in Fig. 16, the relationship between these properties does show some dependence upon the masonry's flexural tensile bond strength. A linear model of this dependence was found to have a coefficient of determination of 0.17.

While this value of a coefficient of determination is still quite low, it may be observed in Fig. 15 that this dependency is more significant at higher flexural tensile bond strengths. In particular, the results presented in this study, and that of Masia et al., [16], indicate that as the flexural tensile bond strength becomes large, the shear bond strength grows less sensitive to the tensile strength, i.e.: the shear bond strength will stop increasing with increases in the flexural tensile bond strength beyond a certain limit. This observation indicates that a log or power law model may produce a better fit than the linear relationship presented in AS 3700 [30] at higher tensile bond strengths.

4.4. Probabilistic descriptions of material relationships

The investigation into the relationships between the flexural tensile bond strength with the direct tensile and shear bond strengths has yielded a large set of experimental data; with 24 and 26 distinct data points describing the flexural to direct tensile strengths and shear to flexural tensile strengths respectively. As such, it is possible to fit, with reasonable confidence, probability distributions to the relationships estimated between these properties. These statistical descriptions may be applied in the stochastic analysis of URM structures. The determination of a suitable probabilistic distribution has been made through the application of the Kolmogorov-Smirnov (K-S) test and the Anderson-Darling (A-D) test, as well as by examining the goodness-of-fit of the Inverse Cumulate Distribution Function (CDF^{-1}), as outlined in the work of Stewart and Lawrence [32]. The probabilistic distributions assessed in this study were: Normal, Lognormal, Weibull, Gamma, and Gumbel distributions.

The initial K-S and A-D tests performed on the proposed probability distributions found that in both cases, none of the models could be rejected at the 5% significance level. As such, analysis of the CDF^{-1} plots was utilised in order to determine the most suitable distribution to describe these material relationships.

The CDF^{-1} of the examined probabilistic models have been assessed based upon how close to the 1:1 line each model fits (see Fig. 17**b** and Fig. 18**b**). A distribution that falls completely along this line would indicate a perfect representation of the experimentally observed data. Additionally, in the case of the ratio between tensile strengths, the upper tail of the probability distributions is of the greatest significance. This is because values at this end of the distribution will correspond to higher ratios between the flexural and direct tensile strengths, and thus will result in a lower direct tensile strength adopted in a stochastic analysis. As such, accuracy in this portion of any adopted probabilistic distribution is more important than in other areas so as to maintain as much conservatism in the selected probabilistic model.

In contrast, the lower tail of the probability distributions describing the ratio between shear and flexural tensile bond strengths is most important as this portion of each probability density function (PDF) corresponds to the lowest estimations of shear strength. These values dictate the shear capacity, and in some cases, failure mechanism of URM walls, and are thus of the greatest significant in the stochastic modelling of URM structures.

In Fig. 17, it may be observed that the Gumbel distribution produces the poorest fit to the data representing the ratio between flexural and direct tensile strengths, while the other distributions fit reasonably well. The lognormal distribution is noted to have the best fit to the upper tail of the CDF^{-1}, as well as having a good fit to the middle and lower

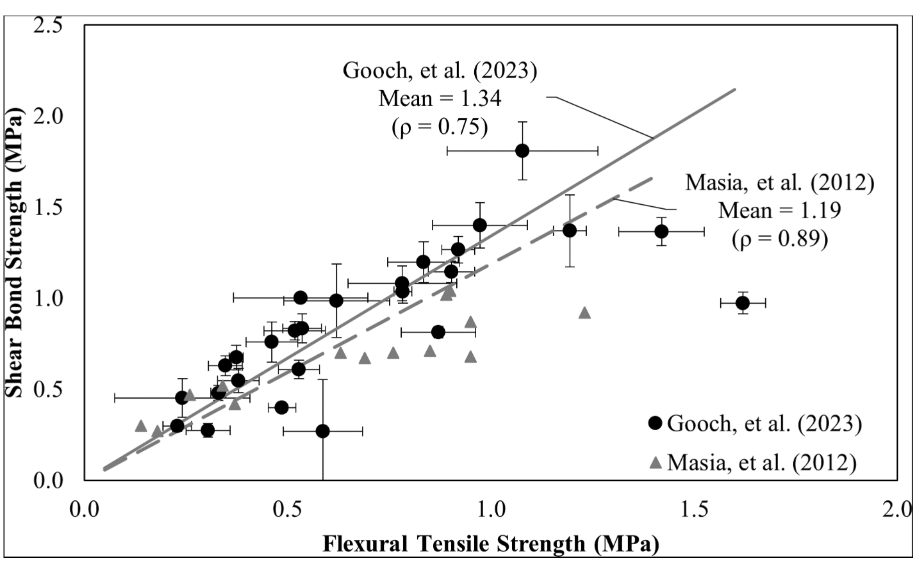

Fig. 15. Comparison of mean flexural tensile and mean shear bond strengths estimated for clay brick masonry with standard error bars shown. The experimentally estimated mean ratio of 1.34 is presented, as well as the results and estimated mean ratio of Masia et al., [16].

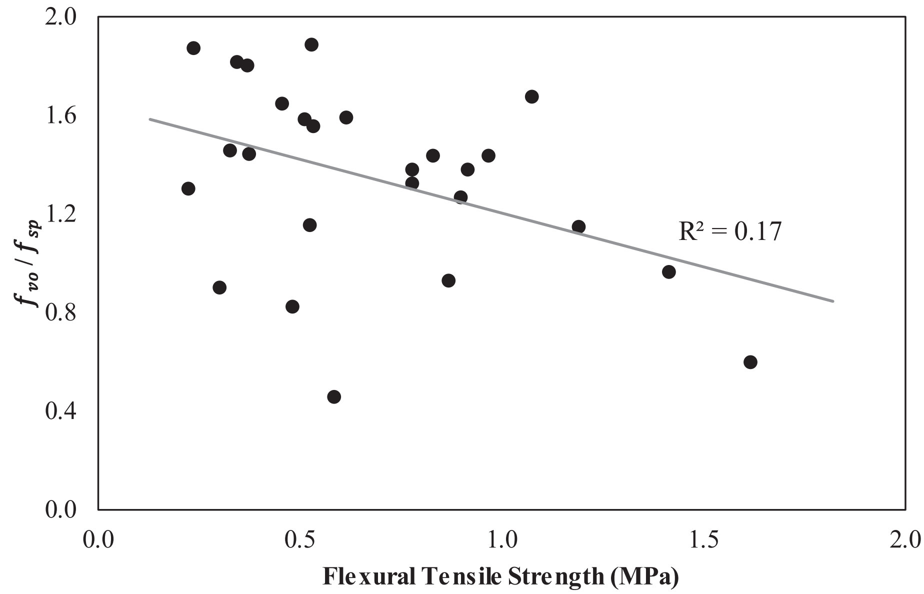

Fig. 16. Comparison between the characteristic flexural tensile bond strength and ratio between characteristic shear and flexural bond strengths.

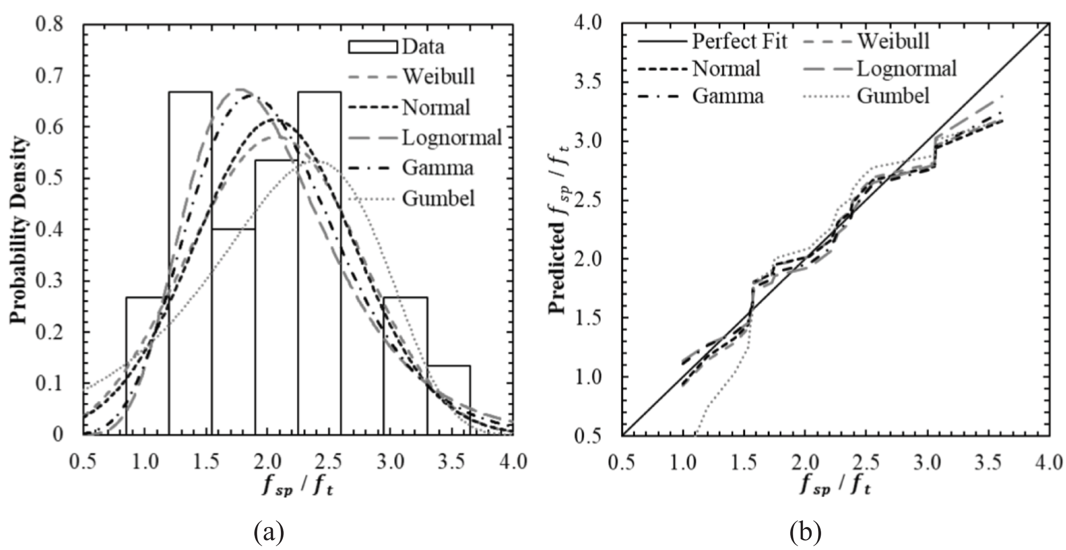

Fig. 17. (a) Probabilistic distributions and (b) Inverse CDF plots of the ratio between flexural tensile and direct tensile bond strengths.

portions.

For Fig. 18, the Gumbel distribution has the best fit to the lower tail of the CDF^{-1}, as well as having only minor deviations from the 1:1 line close to the mean and upper tail of the curve. While other distributions, most notably the Normal and Gamma distributions, fit to the experimental data reasonably well at the tails, the Gumbel distribution maintains the best overall representation of the determined ratios between flexural tensile and shear bond strengths. It should be noted that a Gumbel distribution can be more readily described with a location parameter μ and scale parameter σ, rather than the mean and COV presented in Tables 4 and 5. For the distribution shown in Fig. 18**a**, $\mu = 1.52$ and $\sigma = 0.30$.

Based upon these observations, the probability models determined to be most suitable, along with the relevant means and COVs are presented in Table 5. Note that the mean ratio between flexural and direct tensile strengths of clay brick units is presented here. However, an insufficient amount of data has been produced to assess suitable probabilistic distributions. Further studies into this relationship are planned.

5. Conclusions

A series of experiments were conducted in order to examine the relationships between tensile and shear properties of unreinforced masonry. A mean of 2.06 and a coefficient of variability of 31.5% was estimated for the ratio between flexural and direct tensile bond strengths. Furthermore, through consideration of the best fit of several inverse cumulative density functions, it was found that a lognormal distribution most accurately describes the ratio between these two parameters. Similarly, a mean of 1.34 and a coefficient of variability of 28.4% was determined for the ratio between the shear and flexural tensile bond strengths of mortar joints, with a Gumbel distribution producing the best-fit to the observed data through consideration of several inverse cumulative density functions. Finally, a preliminary estimate of the ratio between the flexural and direct tensile strengths of fired clay bricks has been made, with an estimated mean of 1.29 and coefficient of variability of 14.7%. Further experimental testing is required to validate these results, as well as to draw a reasonable conclusion regarding a suitable probabilistic distribution.

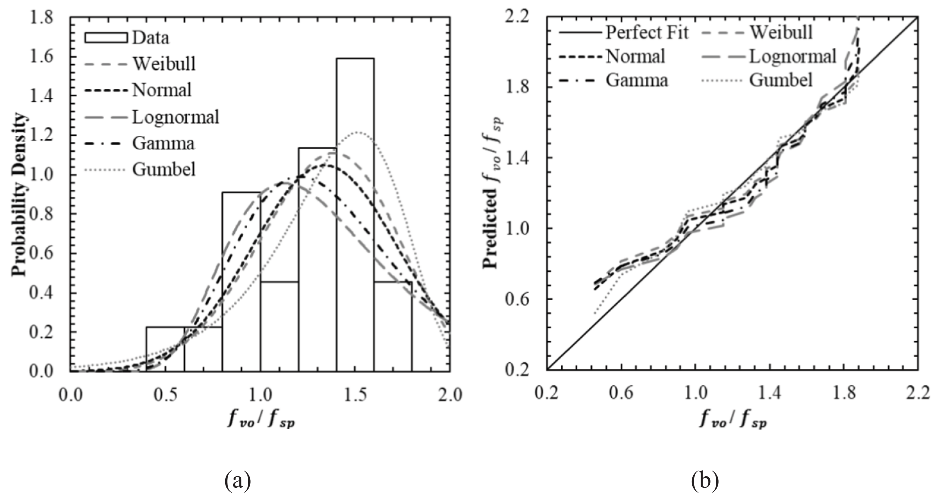

Fig. 18. (a) Probabilistic distributions and (b) Inverse CDF plots of the ratio between shear and flexural tensile bond strengths.

Table 5
Summary of proposed probability distributions.

Variable	Mean	COV	Distribution[1]
Flexural to direct tensile bond strength	2.06	31.5%	Lognormal
Flexural to direct tensile unit strength	1.29	14.7%	–
Shear to flexural tensile bond strength	1.34	28.4%	Gumbel

[1] The mean and COV of the flexural to direct tensile unit strength is summarised here, but insufficient data has been collected in this study to fit a meaningful distribution to these results.

In addition to the above, the degree of correlation between the tensile and shear bond strengths has been estimated in order to assess the validity of the mathematical relationship provided in AS 3700 [30]. A Pearson correlation coefficient of 0.75 was determined, indicating a strong, but not absolute, correlation between the two properties.

CRediT authorship contribution statement

Lewis J. Gooch: Conceptualization, Methodology, Software, Validation, Formal analysis, Investigation, Writing – original draft, Writing – review & editing, Visualization. **Mark J. Masia:** Methodology, Resources, Conceptualization, Validation, Writing – review & editing, Supervision, Project administration, Funding acquisition. **Mark G. Stewart:** Methodology, Resources, Conceptualization, Validation, Writing – review & editing, Supervision, Project administration, Funding acquisition. **Chee Yin Lam:** Investigation.

Declaration of Competing Interest

The authors declare that they have no known competing financial interests or personal relationships that could have appeared to influence the work reported in this paper.

Data availability

Data will be made available on request.

Acknowledgements

The financial support provided by the Australian Research under Council Discovery Project DP180102334 is gratefully acknowledged. The authors are grateful for the assistance provided by the University of Newcastle's laboratory staff and for the experimental work undertaken by undergraduate students, Joel Cook and Samip Dhital.

References

[1] K.F. Abdulla, L.S. Cunningham, M. Gillie, Simulating masonry wall behaviour using a simplified micro-model approach, Eng. Struct. 151 (2017) 249–365.
[2] ASCE, *Seismic Evaluation and Retrofit of Existing Buildings*, American Society of Civil Engineers, Reston, 2014.
[3] British Standards Institution, BS EN1996-1-1: Eurocode 6: Design of Masonry Structures - Part 1–1: General Rules for Reinforced and Unreinforced Masonry Structures, British Standards Institution, London, 2005.
[4] Canadian Standards Association, CSA S304-14: Design of Masonry Structures, Canadian Standards Association, Mississauga, 2014.
[5] DIANA FEA, DIANA 10.3 – User's Manual, DIANA FEA, Delft, 2019.
[6] B. Ellingwood, T.V. Galambos, J.G. MacGregor C.A., Cornell, 1980. *Development of a Probability Based Load Criterion for American National Standard A58.* Special Publication 577 ed. Washington D.C.: National Bureau of Standards.
[7] European Standard, EN1052-3: Methods of Test for Masonry. Part 3: Determination of Initial Shear Strength, European Committee of Standardization, Brussels, 2002.
[8] S. Frumento, G. Magenes, M. Paolo, G.M. Calvi, Interpretation of Experimental Shear Tests on Clay Brick Masonry Walls and Evaluation of q-Factors for Seismic Design, IUSS Press, Pavia, 2009.
[9] L.J. Gooch, M.J. Masia, M.G. Stewart, Application of stochastic numerical analyses in the assessment of spatially variable unreinforced masonry walls subjected to in-plane shear loading, Eng. Struct. 235 (2021) 112095.
[10] M.K. Howlader, M.J. Masia, M.C. Griffith, Numerical analysis and parametric study of unreinforced masonry walls with arch openings under lateral in-plane loading, Eng. Struct. 208 (2020) 110337.
[11] A.C. Isfeld, M.G. Stewart, M.J. Masia, Stochastic finite element model assessing length effect for unreinforced masonry walls subjected to one-way vertical bending under out-of-plane loading, Eng. Struct. 236 (2021) 112115.
[12] K.M.C. Konthesingha, Earthquake Protection of Masonry Shear Walls Using Fibre Reinforced Polymer Strengthening, The University of Newcastle, Australia, Callaghan, 2012.
[13] S.J. Lawrence, Behaviour of Brick Masonry Walls under Lateral Loading, University of New South Wales, Sydney, 1983.
[14] J. Li, M.G. Stewart, M.J. Masia, S.J. Lawrence, Spatial correlation of material properties and structural strength of masonry in horizontal bending, J. Struct. Eng. 142 (11) (2016).
[15] P.B. Lourenço, Computational Strategies for Masonry Structures, Delft University of Technology, Delft, 1996.
[16] M.J. Masia, G. Simundic, A.W. Page, 2012. *Assessment of the AS3700 relationship between shear bond strength and flexural tensile bond strength in unreinforced masonry.* Florianópolis, Proceedings of the 15th International Brick and Block Masonry Conference.
[17] G. Milani, P.B. Lourenço, Simple homogenized model for the nonlinear analysis of FRP-strengthened masonry structures. II: structural applications, J. Eng. Mech. 139 (1) (2013) 77–93.
[18] D. Müller, L. Bujotzek, T. Proske, C.-A. Graubner, Influence of spatially variable material properties on the resistance of masonry walls under compression, Mater. Struct. 55 (2) (2022).
[19] NZSEE, *The Seismic Assessment of Existing Buildings*, Wellington: New Zealand Society for Earthquake Engineering, Structural Engineering Society, and NZ Geotechnical Society, 2017.
[20] R.B. Petersen, N. Ismail, M.J. Masia, J.M. Ingham, Finite element modelling of unreinforced masonry shear wallettes strengthened using twisted steel bars, Constr. Build. Mater. 33 (2012) 14–24.
[21] J.M. Raphael, Tensile strength of concrete, *ACI J.* 81 (2) (1984) 158–165.
[22] J.R. Riddington, A.H. Gambo, G.J. Edgell, 1991. *An assessment of the influence of unit aspect ratio on bond shear strength values given by the proposed CEN triplet test.*

Berlin, Germany, Proceedings of the 9th International Brick/Block Masonry Conference, pp. 1321-1328.

[23] J.R. Riddington, P. Jukes, 1995. *Determination of Material Properties for Use in Masonry FE Analyses.* London, England, Proceedings of 4th International Masonry Conference, pp. 314-319.

[24] Selleys, 2021. *Selleys Araldite Super Strength,* Clayton: Selleys.

[25] T. Siddiquee, accessed 2022. *Brick Size - Standard Brick Dimensions.* [Online] Available at: https://civiltoday.com/civil-engineering-materials/brick/271-brick-size-standard-dimensions.

[26] Standards Australia, Standards New Zealand, 2003. *AS/NZS4456.15: Masonry units, segmental pavers and flags - Methods of test. Method 15: Determining lateral modulus of rupture.* Sydney: Standards Australia, Standards New Zealand.

[27] Standards Australia, AS3600: Concrete Structures, Standards Australia, Sydney, 2009.

[28] Standards Australia, Masonry Structures – Commentary (Supplement to AS 3700: 2011), Standards Australia, Sydney, 2012.

[29] Standards Australia, AS3600: Concrete Structures, Standards Australia, Sydney, 2018.

[30] Standards Australia, AS3700: Masonry Structures, Standards Australia, Sydney, 2018.

[31] Standards New Zealand, NZS4210: Masonry Construction: Material and Workmanship, Standards New Zealand, Wellington, 2001.

[32] M.G. Stewart, S.J. Lawrence, Model error, structural reliability and partial safety factors for structural masonry in compression, Masonry Int. 20 (3) (2007) 107–116.

[33] M.G. Stewart, S.J. Lawrence, Model error and structural reliability for unreinforced masonry walls in vertical bending, Masonry Int. 24 (1) (2011) 23–30.

[34] The Masonry Society, TMS 402/602-16 Building Code Requirements and Specification for Masonry Structures, The Masonry Society, Longmont, 2016.

[35] R. Van der Pluijm, Non-linear behaviour of masonry under tension, Heron 42 (1) (1997) 25–54.